

To appear in Ap. J.

# Viscous Shear Instability in Weakly Magnetized, Dilute Plasmas

Steven A. Balbus<sup>1</sup>

*École Normale Supérieure, Laboratoire de Radioastronomie, 24, rue Lhomond,  
75231 Paris, France*

sb@virginia.edu

## ABSTRACT

When the ion mean free path much exceeds the Larmor radius in a plasma, the viscous stress tensor is altered dramatically, and depends only upon quantities measured along the field lines. This regime corresponds to typical interstellar medium conditions in galaxies and protogalaxies, even if the magnetic field is extremely weak, with a negligible Lorentz force on all scales of interest. In this work, the only role of the magnetic field is to channel angular momentum transport along its lines of force. We show that differential rotation in such a gas is highly unstable, with a maximum growth rate exceeding that of the magnetorotational instability. The regime of interest has been treated previously by plasma kinetic methods. Where there is overlap, our work appears to be in agreement with the kinetic results. The nonlinear outcome of this instability is likely to be a turbulent process, significantly augmenting the magnetorotational instability, and important to the initial phases of the amplification of small galactic magnetic fields.

*Subject headings:* accretion, accretion disks; magnetic fields; MHD; instabilities; galaxies: magnetic fields.

---

<sup>1</sup>permanent address: VITA, Astronomy Department, University of Virginia, Charlottesville, VA 22903

## 1. Introduction

The magnetorotational instability, or MRI, has become central to our understanding of turbulent angular momentum transport in accretion disks (e.g. Balbus 2003). The instability is important even when (indeed, especially when) the magnetic energy density is small compared with the thermal energy density. It is this feature, the fact that the stability of the gas is hypersensitive to the presence of subthermal magnetic fields of any geometry, that endows the MRI with its special significance. In fact, the MRI is merely one manifestation of much more general behavior. By imparting new degrees of freedom to a fluid, magnetic fields allow free energy gradients to become sources of instability, with important consequences for a variety of astrophysical systems: accretion disks become turbulent when the angular velocity (not angular momentum) decreases outward, and stratified dilute gases are destabilized when the temperature (not entropy) decreases upwards (Balbus 2001).

The thermal destabilization caused by magnetic field is especially noteworthy because it is engendered by what seems at first a purely dissipative process: thermal diffusivity. It is the extreme anisotropy of the conductivity tensor parallel and perpendicular to the field lines that lies at the heart of the instability. By channeling heat only along lines of magnetic force, small-amplitude ripples along initially isothermal field lines grow into large fluid displacements parallel to the temperature gradient. This is not, as is sometimes thought, analogous to classical double-diffusive instabilities, such as ocean layer “salt-fingering”<sup>1</sup>. Rather, it depends wholly upon the properties of anisotropic conductivity.

In this paper we show that the anisotropy introduced into the viscous stress tensor by a weak magnetic field sharply destabilizes dilute astrophysical disks, even without Lorentz forces appearing in the fluid equations. By “dilute,” we mean the limit in which the ion Larmor radius is small compared to a mean free path, which in turn is small compared with the characteristic macroscopic length scales of the disk. We shall refer to the resulting viscous stress tensor in this limit as Braginskii viscosity (Braginskii 1965). The Braginskii limit is appropriate for interstellar and galactic disks (especially protogalactic disks, cf. Malyshkin & Kulsrud 2002). A remarkable property of the instability is that in the absence of Lorentz forces, when the viscous diffusivity much exceeds the resistive diffusivity, rapid growth times are associated with arbitrarily high wave numbers. Except for isolated field geometries (e.g. precisely azimuthal), there is no formal high wavenumber dissipation of the linear magneto-viscous instability. By way of contrast, for the ultra-weak magnetic fields considered here, the wavelength of maximum growth in the classical MRI would be strongly damped by an ordinary isotropic viscosity. (Note that in real systems, at sufficiently high wave numbers,

---

<sup>1</sup>See Menou, Balbus, & Spruit (2004) for a true salt-fingering analogy involving the MRI.

Lorentz forces will ultimately stabilize.)

The magnetic stability of a dilute plasma may also be studied using a plasma kinetic approach. This offers rigor in a problem where it is clearly of some benefit, but at a price of greater mathematical complexity. Quataert, Dorland, & Hammett (2002) analyzed the MRI in the collisionless regime, and noted that the character of the instability changes when the pressure tensor becomes significantly anisotropic, with growth rates in excess of the classical MRI maximum. In the current work, we have in essence abstracted the anisotropic components of the pressure, and labeled them as a viscosity tensor. More recently, Sharma, Hammett & Quataert (2003) reanalyzed the kinetic problem using a Krook collision operator, and showed that the collisional and collisionless behavior are on the same branch of the dispersion relation. In the short mean free path limit, the pressure tensor associated with the equations used by Sharma et al. 2003 reduces to a scalar pressure plus the dominant parallel components of the Braginskii viscosity (Snyder, Hammett, & Dorland 1997). The current work, a purely gasdynamical treatment of the problem, affords relative mathematical simplicity and a physically transparent interpretation.

In either its kinetic or gasdynamical guise, this vigorous instability may be important in the early stages of magnetic field amplification in disk galaxies, when densities are low, temperatures are relatively high, and the field is likely to be very weak. Quataert et al. (2002) and Sharma et al. (2003) discuss applications to black hole accretion flows of low radiative efficiency.

An outline of the paper is as follows. Section 2 is a discussion of the regime of the applicability of this work and a presentation of the magnetic viscosity formalism. Section 3 is the heart of the paper, formulating and solving the problem, and checking the validity of the results. Section 4 is a discussion of the applicability of our results to galactic magnetism, and section 5 summarizes our findings.

## 2. Preliminaries

### 2.1. Gasdynamical Description of the Instability

We begin with a physical description of the instability. The process is very simple. In the leftmost diagram of figure 1 (a), we show three representative azimuthal field lines, with increasing azimuth toward the top. The angular velocity gradient  $\nabla\Omega$  is radial, pointing from right to left, so that smaller angular velocities lie to the right. The angular momentum gradient, by contrast, runs from left to right. Initially, there is no viscous transport of angular momentum, because the angular velocity gradient and field lines are orthogonal.

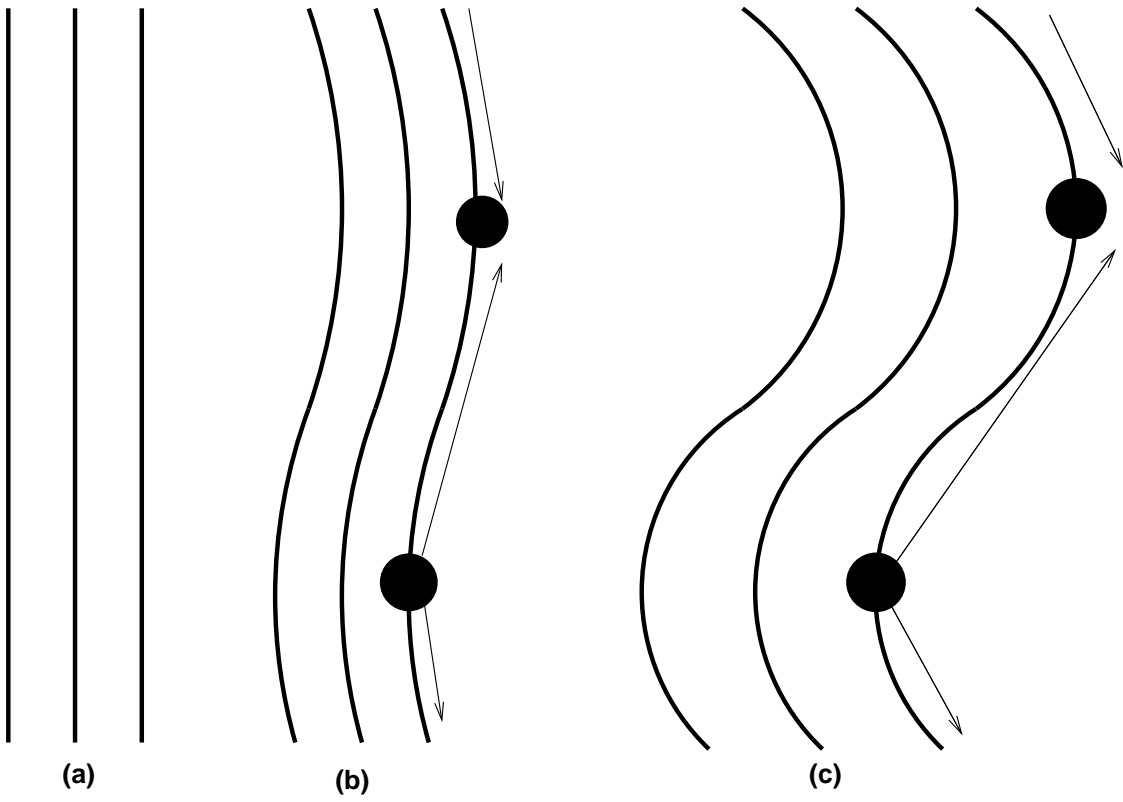


Fig. 1.— Development of magneto-viscous instability in three stages. See text for details.

The middle portion of figure 1 (b) shows the field lines and two fiducial fluid elements (dark circular disks) after a perturbation has created a small oscillatory radial component. Now there is a component of  $\nabla\Omega$  along the field lines, and viscous angular momentum transport, represented by the thin arrows, is able to commence. The rightward fluid element acquires angular momentum, while the leftward element loses angular momentum.

In the rightmost portion of the figure (c), the loss of angular momentum causes the element on the left to fall further leftward, towards orbits of smaller angular momentum. The element on the right, on the other hand, acquires angular momentum, and moves toward the higher angular momentum orbits that lie further to the right. The critical point is that these dynamical motions stretch the field lines yet more radially, allowing yet more angular momentum to flow between the elements, and the process runs away.

The instability blends different aspects of previously known instabilities. It works on the same dynamical principles as the MRI, tethering fluid elements and transporting angular momentum between them, but there is no magnetic tension here. Similarly, it works using the same gradient transport process seen in the magneto-thermal instability, channeling diffusive transport along magnetic field lines while simultaneously realigning them, but with angular momentum rather than heat. The result of all this, we shall see, is an extremely powerful shear instability.

## 2.2. Dilute Plasma Limit

The presence of a magnetic field alters the form of the viscosity when

$$\epsilon \equiv (\omega_{ci}\tau_{ci})^{-1} \ll 1, \quad (1)$$

where  $\omega_{ci}$  is the ion cyclotron frequency and  $\tau_{ci}$  is the ion-ion mean collision time. (This is tantamount to having the mean free path much exceed the gyroradius.) Under laboratory conditions, this is normally considered to be the large field strength limit, but it is very much the norm for interstellar plasmas, even when the field is very weak. Indeed, reference to Spitzer (1962) gives for a hydrogenic plasma

$$\omega_{ci}\tau_{ci} = \left( \frac{1.09 \times 10^5}{n} \right) \frac{T_4^{3/2} B_{\mu G}}{\ln \Lambda}, \quad (2)$$

where  $n$  is the proton density in  $\text{cm}^{-3}$ ,  $T_4$  the kinetic temperature in units of  $10^4$  K,  $B_{\mu G}$  is the magnetic field in microgauss, and  $\ln \Lambda$  is the Coulomb logarithm,  $\sim 20$ . With  $n \lesssim 1$  and  $T_4 \gtrsim 1$ , very weak fields are clearly accommodated by the asymptotic regime  $\epsilon \ll 1$ . The

ion mean free path  $\lambda_{mfp}$  and gyroradius  $r_g$  are respectively

$$\lambda_{mfp} = 5.2 \times 10^{11} \left( \frac{20}{\ln \Lambda} \right) \left( \frac{T_4^2}{n} \right) \text{ cm}, \quad r_g = 1.3 \times 10^8 \left( \frac{T_4^{1/2}}{B_{\mu G}} \right) \text{ cm}. \quad (3)$$

### 2.3. Ideal MHD Limit

Throughout this work, we ignore the effects of finite resistivity. The ratio of the viscosity to resistivity is known as the magnetic Prandtl number  $\mathcal{P}$ , and may be adapted from Balbus & Hawley (1998):

$$\mathcal{P} = \left( \frac{T}{10^4} \right)^4 \left( \frac{6.5 \times 10^{10}}{n} \right) \left( \frac{20}{\ln \Lambda} \right)^2. \quad (4)$$

We may easily restrict the calculations to  $T \gtrsim 10^4$  K and  $n \ll 10^{10} \text{ cm}^{-3}$ , so that  $\mathcal{P} \gg 1$ , and resistivity will be ignored. Since these questions can be subtle however, we return to this point *ex post facto* in §3.5.

### 2.4. Magnetic Viscous Stress Tensor

The theory of viscous transport in magnetized plasmas is presented by Braginskii (1965). The usual isotropic collisional viscous stress tensor can be written

$$\sigma_{ij} = -\eta W_{ij}, \quad (5)$$

where  $\eta$  is the dynamical viscosity coefficient, and

$$W_{ij} = \frac{\partial v_i}{\partial x_j} + \frac{\partial v_j}{\partial x_i} - \frac{2}{3} \delta_{ij} \nabla \cdot \mathbf{v}. \quad (6)$$

This form applies to a set of Cartesian axes,  $(i, j, k)$  being an even permutation of  $(X, Y, Z)$ . As usual,  $\delta_{ij}$  denotes the Kronecker delta function. We note that the stress is traceless. In the paper, we work exclusively in the Boussinesq limit, and shall set  $\nabla \cdot \mathbf{v} = 0$  in the above. In §3.4, it is shown that the Boussinesq limit is justified when the Reynolds number is large.

In the presence of a restricting magnetic field, the only component of  $\sigma_{ij}$  that remains unaffected is the momentum flux along the magnetic line of force due to the gradient along the field line. Define a local Cartesian coordinate system (the “field frame”)  $(X_b, Y_b, Z_b)$ , chosen with the magnetic field lying along the  $Z_b$  axis. Then

$$\sigma_{Z_b Z_b} = \sum_{i,j} b_i b_j \sigma_{ij}, \quad (7)$$

where the  $b_i$  are components of the unit magnetic field vector in an arbitrary Cartesian frame. Braginskii (1965) shows that all other components of the magnetized viscous stress tensor are smaller than  $\sigma_{Z_b Z_b}$  by a factor of order  $\epsilon$  or  $\epsilon^2$ , and are therefore ignored in this calculation. The important exception are the two other diagonal stress components, which to leading order in  $\epsilon$  are identical with one another. Since the stress must always be traceless, we have

$$\sigma_{X_b X_b} = \sigma_{Y_b Y_b} = -\frac{1}{2}\sigma_{Z_b Z_b}. \quad (8)$$

In vector notation, the  $Z_b Z_b$  component of the stress is then given by

$$\sigma_{Z_b Z_b} = -2\eta [(\mathbf{b} \cdot \nabla) \mathbf{v}] \cdot \mathbf{b}. \quad (9)$$

To find the components of the magnetized viscous stress tensor in any other locally Cartesian frame, the transformation law may be written

$$\sigma_{ij} = \sum_{i_b, j_b} (\mathbf{i} \cdot \mathbf{i}_b) (\mathbf{j} \cdot \mathbf{j}_b) \sigma_{i_b j_b}, \quad (10)$$

where once again the  $b$  subscript denotes the magnetic field frame and bold face quantities are unit vectors of the indicated component. Using equation (8) for the nonvanishing diagonal stress tensor components in the field frame, we find

$$\sigma_{ij} = \sigma_{Z_b Z_b} \left[ (\mathbf{i} \cdot \mathbf{Z}_b)(\mathbf{j} \cdot \mathbf{Z}_b) - \frac{1}{2}(\mathbf{i} \cdot \mathbf{Y}_b)(\mathbf{j} \cdot \mathbf{Y}_b) - \frac{1}{2}(\mathbf{i} \cdot \mathbf{X}_b)(\mathbf{j} \cdot \mathbf{X}_b) \right]. \quad (11)$$

Equations (9) and (11) allow one to determine the magnetic viscous stress in a frame suitable for working with fluid variables, given the local field geometry.

### 3. Formulation of the Problem

We consider the stability of a disk in the presence of a magnetic field, but with a field so weak that all dynamical magnetic forces are negligibly small. In contrast to the MRI, we assume this “magneto-anemic” condition is true not only for the equilibrium disk, but even for small wavelength, WKB perturbations. The sole effect of the magnetic field is to restrict viscous transport in accordance with prescription of §2.

The fundamental fluid equations used here are mass conservation

$$\frac{\partial \rho}{\partial t} + \nabla \cdot (\rho \mathbf{v}) = 0, \quad (12)$$

the equation of motion,

$$\rho \left( \frac{\partial}{\partial t} + \mathbf{v} \cdot \nabla \right) \mathbf{v} = -\nabla P - \rho \nabla \Phi - \frac{\partial \sigma_{ij}}{\partial x_j}, \quad (13)$$

and the induction equation of ideal MHD,

$$\frac{\partial \mathbf{B}}{\partial t} = \nabla \times (\mathbf{v} \times \mathbf{B}). \quad (14)$$

For reasons that will become clear, an internal energy equation is not needed at this stage.

The equilibrium state is a differentially rotating disk, and we work in the usual cylindrical coordinate system,  $R, \phi, Z$ . The angular velocity is  $\Omega(R)$ , and we shall restrict ourselves to a local analysis at the midplane. Thus, we may ignore buoyant forces, which depend upon gradients in pressure and entropy.

In the equilibrium state, it is assumed that  $\sigma_{ij} = 0$ . Indeed, the point of this calculation is to show that any development of viscous transport along a field line is highly unstable. The initial magnetic field lines are wrapped around cylinders, and are unaffected by the shear.

We consider next small departures from the equilibrium flow. Linearly perturbed quantities are denoted by  $\delta \mathbf{v}, \delta \sigma_{ij}$ , etc. We work in the local WKB limit, with the space-time dependence of all perturbed quantities given by  $\exp(\gamma t + i \mathbf{k} \cdot \mathbf{r})$ . Thus,  $\gamma$  is a growth or decay rate if it is real, and an angular frequency if it is imaginary.

The wavenumber  $\mathbf{k}$  as well as the assumed constancy of  $\gamma$  require some further explanation. The wavenumber has radial, azimuthal and vertical components  $k_R, m/R, k_Z$  respectively. Since we are working in a local shearing system, the radial wavenumber  $k_R$  will formally depend on time (Goldreich & Lynden-Bell 1965; Balbus & Hawley 1992):

$$k_R(t) = k_R(0) - mt \frac{d\Omega}{d \ln R}, \quad (15)$$

where  $k_R(0)$  is the initial value of  $k_R$ . For our present purposes however, the time dependence of  $k_R$  will prove irrelevant, as the radial wavenumber disappears early in the analysis. It is for this reason that we may also assume a simple exponential time dependence; in general the problem is more complex.

To evaluate  $\delta \sigma_{ij}$ , it follows from equation (11) that

$$\delta \sigma_{ij} = \delta \sigma_{Z_b Z_b} \left[ (\mathbf{i} \cdot \mathbf{Z}_b)(\mathbf{j} \cdot \mathbf{Z}_b) - \frac{1}{2}(\mathbf{i} \cdot \mathbf{Y}_b)(\mathbf{j} \cdot \mathbf{Y}_b) - \frac{1}{2}(\mathbf{i} \cdot \mathbf{X}_b)(\mathbf{j} \cdot \mathbf{X}_b) \right], \quad (16)$$

since  $\sigma_{Z_b Z_b}$  vanishes in the unperturbed state. The terms in square brackets may be evaluated for the equilibrium field geometry, which we take to be

$$\mathbf{b} = \cos \theta \hat{\phi} + \sin \theta \hat{\mathbf{Z}}. \quad (17)$$



$\hat{\phi}$ ,  $\hat{Z}$ , and  $\hat{R}$  are unit vectors in the indicated cylindrical directions, and  $\theta$  is the angle between the magnetic field and the  $\phi$  axis. The local magnetic field axes are then

$$\mathbf{Z}_b = \mathbf{b} = \cos \theta \hat{\phi} + \sin \theta \hat{Z}, \quad (18)$$

$$\mathbf{X}_b = \hat{R} \times \mathbf{Z}_b = -\sin \theta \hat{\phi} + \cos \theta \hat{Z}, \quad (19)$$

and

$$\mathbf{Y}_b = \hat{R}. \quad (20)$$

See fig. 2.

The nonvanishing elements of  $\delta\sigma_{ij}$  may now be calculated. The diagonal elements are

$$\delta\sigma_{RR} = -\frac{1}{2}\delta\sigma_{Z_b Z_b}, \quad \delta\sigma_{\phi\phi} = \left(\cos^2 \theta - \frac{\sin^2 \theta}{2}\right) \delta\sigma_{Z_b Z_b}, \quad \delta\sigma_{ZZ} = \left(\sin^2 \theta - \frac{\cos^2 \theta}{2}\right) \delta\sigma_{Z_b Z_b}, \quad (21)$$

and the off-diagonal elements are

$$\delta\sigma_{\phi Z} = \delta\sigma_{Z\phi} = \frac{3}{2} \cos \theta \sin \theta \delta\sigma_{Z_b Z_b}. \quad (22)$$

We may evaluate  $\delta\sigma_{Z_b Z_b}$  from its vector-invariant form (9),

$$\delta\sigma_{Z_b Z_b} = -2\eta \left( [(\delta\mathbf{b} \cdot \nabla) \mathbf{v}] \cdot \mathbf{b} + [(\mathbf{b} \cdot \nabla) \delta\mathbf{v}] \cdot \mathbf{b} + [(\mathbf{b} \cdot \nabla) \mathbf{v}] \cdot \delta\mathbf{b} \right). \quad (23)$$

Using  $\mathbf{v} = R\Omega\hat{\phi}$  and equation (18), we find

$$\delta\sigma_{Z_b Z_b} = -2\eta \left[ \delta b_R \frac{d\Omega}{d \ln R} \cos \theta + i(\mathbf{k} \cdot \mathbf{b})(\mathbf{b} \cdot \delta\mathbf{v}) \right]. \quad (24)$$

### 3.1. Linearized Equations

The linearized equations are written in a coordinate system that is shearing with the unperturbed flow. The only effects this has on the equations of motion are that the time derivative must be Lagrangian,

$$\frac{d}{dt} \equiv \frac{\partial}{\partial t} + \Omega \frac{\partial}{\partial \phi}, \quad (25)$$

and the radial partial derivative is replaced by the  $k_R(t)$  wavenumber in equation (15) (Balbus & Hawley 1992). The dynamical equations are

$$\mathbf{k} \cdot \delta\mathbf{v} = 0, \quad (26)$$

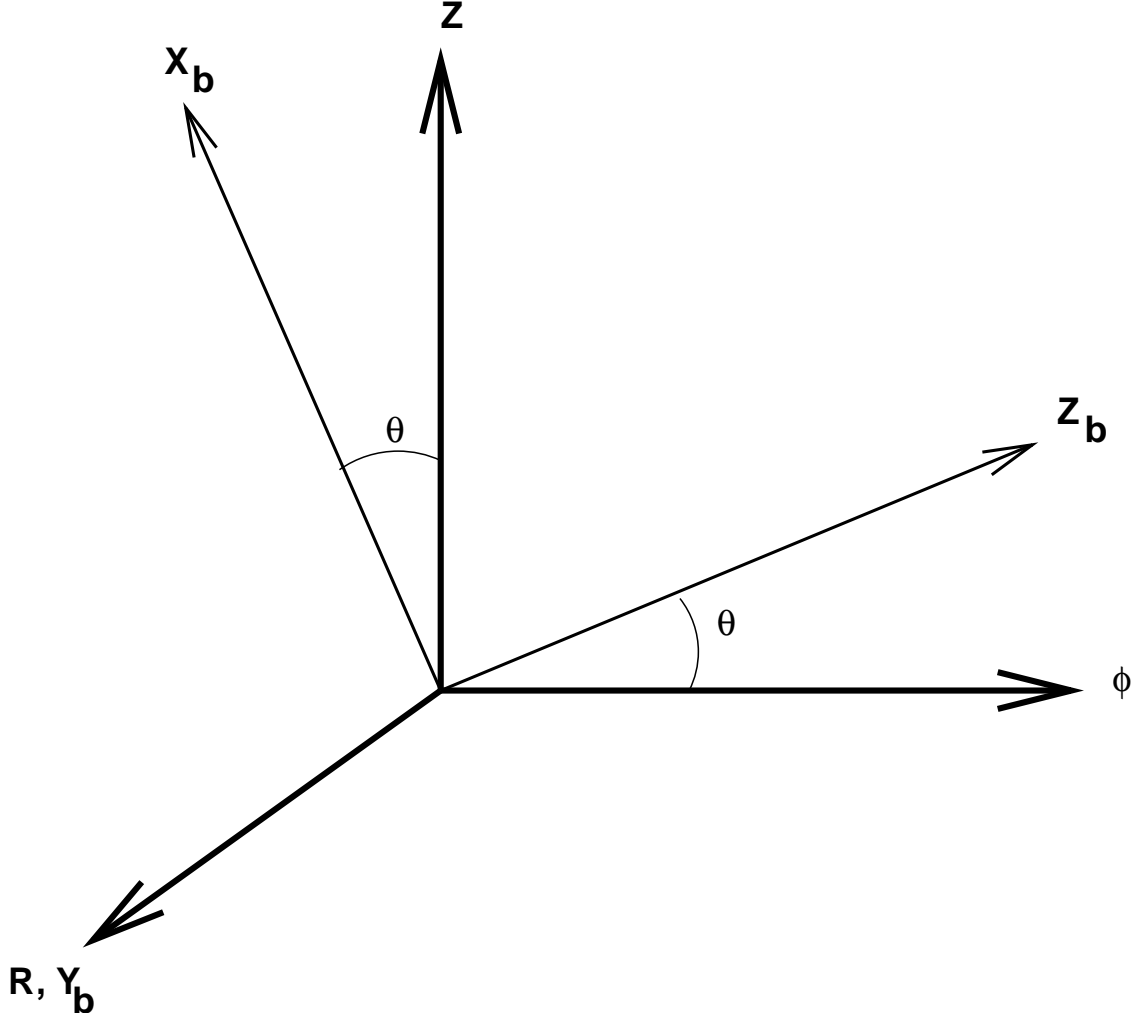


Fig. 2.— Relative orientation of cylindrical  $R, \phi, Z$  and magnetic  $X_b, Y_b, Z_b$  axes. Magnetic field lies along  $Z_b$ , and  $R$  and  $Y_b$  axes coincide.

$$\frac{d\delta v_R}{dt} - 2\Omega\delta v_\phi + \frac{ik_R}{\rho} \left( \delta P - \frac{\delta\sigma_{Z_b Z_b}}{2} \right) = 0, \quad (27)$$

$$\frac{d\delta v_\phi}{dt} + \frac{\kappa^2}{2\Omega}\delta v_R + i\frac{m}{\rho R} \left[ \delta P + \left( \cos^2 \theta - \frac{\sin^2 \theta}{2} \right) \delta\sigma_{Z_b Z_b} \right] + i\frac{3k_Z}{2\rho} \sin \theta \cos \theta \delta\sigma_{Z_b Z_b} = 0, \quad (28)$$

$$\frac{d\delta v_Z}{dt} + \frac{ik_Z}{\rho} \left[ \delta P + \left( \sin^2 \theta - \frac{\cos^2 \theta}{2} \right) \delta\sigma_{Z_b Z_b} \right] + i\frac{3m}{2\rho R} \sin \theta \cos \theta \delta\sigma_{Z_b Z_b} = 0. \quad (29)$$

In equation (28), we have introduced the standard notation  $\kappa$  for the epicyclic frequency, which characterizes the response of fluid element displacements in the  $R\phi$  plane in a non-magnetized disk. In terms of the angular velocity  $\Omega(R)$ ,

$$\kappa^2 = 4\Omega^2 + \frac{d\Omega^2}{d \ln R}. \quad (30)$$

Notice that only the perturbed radial component of the magnetic field unit vector  $\delta b_R$  is required in  $\delta\sigma_{Z_b Z_b}$ . This is easily obtained from the radial induction equation:

$$\frac{d\delta b_R}{dt} = i(\mathbf{k} \cdot \mathbf{b}) \delta v_R. \quad (31)$$

When the time dependence of the perturbations is a simple exponential, this immediately gives

$$\delta b_R = \frac{i(\mathbf{k} \cdot \mathbf{b})}{\gamma} \delta v_R, \quad (32)$$

and

$$\delta\sigma_{Z_b Z_b} = -2\eta i(\mathbf{k} \cdot \mathbf{b}) \cos \theta \left[ \frac{\delta v_R}{\gamma} \frac{d\Omega}{d \ln R} + \delta v_\phi \right] - 2\eta i(\mathbf{k} \cdot \mathbf{b}) \sin \theta \delta v_Z. \quad (33)$$

### 3.2. Axisymmetric Disturbances

If there are both vertical and azimuthal field components present, the problem admits a relatively simple axisymmetric solution with  $\mathbf{k}$  having only a vertical component. This is also likely to be the most unstable mode, and therefore of greatest astrophysical interest.

With  $\mathbf{k} = k_Z \hat{\mathbf{z}}$ , mass conservation immediately gives  $\delta v_Z = 0$ . The remaining dynamical equations are

$$\frac{d\delta v_R}{dt} - 2\Omega\delta v_\phi = 0, \quad (34)$$

$$\frac{d\delta v_\phi}{dt} + \frac{\kappa^2}{2\Omega}\delta v_R + \frac{3}{2\rho} ik_Z \sin \theta \cos \theta \delta\sigma_{Z_b Z_b} = 0, \quad (35)$$

$$\delta P + \left( \sin^2 \theta - \frac{\cos^2 \theta}{2} \right) \delta \sigma_{Z_b Z_b} = 0. \quad (36)$$

Equation (36) is one of vertical hydrostatic equilibrium. In an adiabatic gas, this constraint must be consistent with the Boussinesq approximation, a point we revisit in §3.4.

The problem decouples, and we are simply left with the two equations (34) and (35) for  $\delta v_R$  and  $\delta v_\phi$ . We may seek solutions with an exponential time dependence of the form  $\exp(\gamma t)$ . Then

$$\frac{\delta \sigma_{Z_b Z_b}}{\rho} = -2\nu i k_Z \sin \theta \cos \theta \left( \frac{d\Omega}{d \ln R} \frac{\delta v_R}{\gamma} + \delta v_\phi \right), \quad (37)$$

where we have introduced the kinematic viscosity,

$$\nu \equiv \frac{\eta}{\rho}. \quad (38)$$

Substituting this into equations (34) and (35) yields the dispersion relation

$$\gamma^3 + (3\nu k_Z^2 \sin^2 \theta \cos^2 \theta) \gamma^2 + \kappa^2 \gamma + 3\nu k_Z^2 \sin^2 \theta \cos^2 \theta \frac{d\Omega^2}{d \ln R} = 0. \quad (39)$$

This may be written

$$3\nu k_Z^2 \sin^2 \theta \cos^2 \theta = -\frac{\gamma(\gamma^2 + \kappa^2)}{\gamma^2 + d\Omega^2/d \ln R}, \quad (40)$$

from which it is clear there is an unstable branch ( $\gamma > 0$ ) of the dispersion relation if  $\gamma + d\Omega^2/dR < 0$ . The maximum growth rate is

$$\gamma_{max}^2 = -\frac{d\Omega^2}{d \ln R}. \quad (41)$$

It is noteworthy that  $\gamma$  may exceed the Oort A value  $(1/2)|d\Omega/d \ln R|$ , a result emphasized by Quataert et al. (2002) for a collisionless gas, who also recovered equation (41) in the appropriate limit. We note here the interesting fact that the growth rate given in (41) will always exceed the Oort A value in any disk that is locally stable by the Rayleigh criterion. Equations (34) and (35) may be compared with equations (34) and (35) of Quataert et al. (2002). Note in particular the identification of the  $\phi Z$  component of the viscous stress tensor with the term proportional to  $\delta p_{\parallel} - \delta p_{\perp}$  on the right side of equation (35) of Quataert et al. (2002). In both the kinetic and gasdynamical treatment, the azimuthal torque has no stabilizing radial counterpart, which is responsible for the the resulting growth rate exceeding the classical MRI Oort A value.

For a typical flat galactic rotation curve, the above gives  $\gamma_{max} = \sqrt{2}\Omega$ . This is an enormous rate: linear amplitudes grow a factor of  $7.2 \times 10^3$  in one orbit,  $5.2 \times 10^7$  in two orbits. We have of course neglected magnetic tension, which would ultimately be a stabilizing

influence, but not before it was a powerful destabilizing influence in the form of the MRI. A general treatment including the dynamical effects of the field is deferred to a forthcoming paper. But our finding certainly suggests that a kinematic treatment of field amplification in galactic disks is at best questionable. For plasma kinetic treatments including Lorentz forces, see Quataert et al. (2002) and Sharma et al. (2003).

### 3.3. Azimuthal Field Instability

The above analysis depended upon both axial and azimuthal field components being present. It is of interest to isolate the case of an exactly azimuthal field ( $\theta = 0$ ) and examine its stability properties.

We assume that the wave vector is dominated by its axial component; however, in contrast to the previous section, we do not set the azimuthal and radial components to zero. Rather, we work in the asymptotic limit

$$k_Z \gg k_R(0), m/R. \quad (42)$$

The dynamical equations of motion in this case are

$$\frac{d\delta v_R}{dt} - 2\Omega\delta v_\phi + \frac{ik_R}{\rho} \left( \delta P - \frac{\delta\sigma_{Z_b Z_b}}{2} \right) = 0, \quad (43)$$

$$\frac{d\delta v_\phi}{dt} + \frac{\kappa^2}{2\Omega}\delta v_R + i\frac{m}{\rho R} (\delta P + \delta\sigma_{Z_b Z_b}) = 0, \quad (44)$$

$$\frac{d\delta v_Z}{dt} + \frac{ik_Z}{\rho} \left( \delta P - \frac{\delta\sigma_{Z_b Z_b}}{2} \right) = 0. \quad (45)$$

Mass conservation  $\mathbf{k} \cdot \delta \mathbf{v} = 0$  implies that  $\delta v_Z$  is of order  $1/k_Z$  relative to the planar velocity components, and equation (45) simplifies to

$$\delta P - \delta\sigma_{Z_b Z_b} = 0. \quad (46)$$

The remaining dynamical equations are

$$\frac{d\delta v_R}{dt} - 2\Omega\delta v_\phi = 0, \quad (47)$$

$$\frac{d\delta v_\phi}{dt} + \frac{\kappa^2}{2\Omega}\delta v_R + i\frac{m}{\rho R} \left( \frac{3}{2}\delta\sigma_{Z_b Z_b} \right) = 0. \quad (48)$$

Once again, the radial wavenumber  $k_R$  has dropped from the problem (as has the dominant component  $k_Z$ ), and we may look for simple exponential time behavior of the form  $e^{\gamma t}$ . We find

$$\delta\sigma_{Z_b Z_b} = -2i\eta \frac{m}{R} \left[ \frac{\delta v_R}{\gamma} \frac{d\Omega}{d \ln R} + \delta v_\phi \right]. \quad (49)$$

But this is exactly the problem we solved in the previous section, with the substitution

$$k_Z \sin \theta \cos \theta \leftarrow m/R. \quad (50)$$

We obtain exactly the same dispersion relation,

$$\gamma^3 + 3\gamma^2 \nu m^2 / R^2 + \kappa^2 \gamma + 3\nu(m^2 / R^2) \frac{d\Omega^2}{d \ln R} = 0, \quad (51)$$

and thus exactly the same maximum growth rate,  $|d\Omega^2/d \ln R|$ .

### 3.4. Validity of the Boussinesq Approximation

The Boussinesq approximation was very important for simplifying the preceding analyses. We review its validity here.

The key point is that the perturbed pressure is of order

$$\delta P \sim \delta\sigma_{Z_b Z_b} \sim (\mathbf{k} \cdot \mathbf{b}) \eta \delta v_\phi, \quad (52)$$

since  $\delta v_R$  and  $\delta v_\phi$  are comparable and the growth rates are of order  $\Omega$ . Assuming that any radial entropy gradient is very small,

$$\frac{\delta \rho}{\rho} \sim \frac{\delta P}{P} \sim \frac{\delta P}{\rho c_S^2}, \quad (53)$$

where  $c_S$  is the isothermal sound speed. Hence

$$\frac{\delta \rho}{\rho} \sim \frac{\nu(\mathbf{k} \cdot \mathbf{b})}{c_S} \frac{\delta v_\phi}{c_S}. \quad (54)$$

The Boussinesq approximation requires

$$\frac{d \ln \rho}{dt} \sim \Omega \frac{\delta \rho}{\rho} \ll k \delta v, \quad (55)$$

where  $k$  and  $\delta v$  are respectively characteristic values for the wave number and perturbed velocity. With  $k \sim \mathbf{k} \cdot \mathbf{b}$ , this requirement simplifies to

$$\frac{\nu}{(c_S^2/\Omega)} \ll 1. \quad (56)$$

The quantity on the left is  $1/Re$ , the inverse of the Reynolds number. The Boussinesq limit is therefore generally appropriate for our problem in the limit of large Reynolds number.

### 3.5. Effect of Resistivity

A finite resistivity will always be present, directly affecting the dynamics because of its role in modifying the constraint of field freezing. The question arises as to whether resistivity may generally be ignored at all wavenumbers if the viscous diffusivity  $\nu$  much exceeds the resistive diffusivity  $\eta_B$ . (Unlike the transformation of the viscous stress tensor, the parallel and transverse resistivities do not differ profoundly [Spitzer 1962], and we shall ignore the distinction here.)

The presence of Ohmic resistance alters equation (32) to

$$b_R = \frac{i(\mathbf{k} \cdot \mathbf{b})}{\gamma + \eta_B k^2} \delta v_R, \quad (57)$$

where  $k^2$  is the magnitude of the wavenumber. In both of our worked examples,  $k$  may be taken as  $k_Z$ .

It is a straightforward exercise to rework the dispersion formula using the above for  $b_R$ . One obtains for the case of axisymmetric disturbances,

$$\begin{aligned} & \gamma^3 + \gamma^2 k_Z^2 (\eta_B + 3\nu \sin^2 \theta \cos^2 \theta) + \gamma(\kappa^2 + 3\eta_B \nu k_Z^4 \sin^2 \theta \cos^2 \theta) + \\ & + k_Z^2 \left( \eta_B \kappa^2 + 3\nu \sin^2 \theta \cos^2 \theta \frac{d\Omega^2}{d \ln R} \right) = 0. \end{aligned} \quad (58)$$

As an equation for  $k_Z^2$  this reads

$$\begin{aligned} & 3k_Z^4 (\gamma \eta_B \nu \sin^2 \theta \cos^2 \theta) + k_Z^2 [\eta_B (\gamma^2 + \kappa^2) + 3\nu \sin^2 \theta \cos^2 \theta (\gamma^2 + d\Omega^2/d \ln R)] + \\ & + \gamma(\gamma^2 + \kappa^2) = 0. \end{aligned} \quad (59)$$

For  $\gamma > 0$ , positive solutions for  $k_Z^2$  exist only if the coefficient of  $k_Z^2$  is negative, which, in the limit  $\nu \gg \eta_B$ , requires  $d\Omega^2/dR < 0$  as before. The quadratic discriminant in the solution for  $k_Z^2$  must also be positive. If we set

$$\gamma^2 + \frac{d\Omega^2}{d \ln R} = \epsilon \frac{d\Omega^2}{d \ln R}, \quad (60)$$

and assume that  $\epsilon \ll 1$ , the condition for the positivity of the discriminant is easily worked out. We find

$$\epsilon^2 > \frac{64\eta_B}{3\nu \sin^2(2\theta)} \left| \frac{d \ln \Omega^2}{d \ln R} \right|^{-1}. \quad (61)$$

Provided that  $\theta$  is not too small, this is consistent with our small  $\epsilon$  assumption, and shows that a small resistivity will not strongly alter the conclusions of §3.2.

For the case of an azimuthal magnetic field, the above breaks down and a separate analysis is needed. There is, already at the start, a small parameter in the problem:  $m/k_Z R$ . The requirement that that resistivity be negligible is not satisfied merely by  $\eta_B \ll \nu$ , but by the tighter restriction

$$\eta_B \ll 3\nu(m/k_Z R)^2. \quad (62)$$

This is seen explicitly in the dispersion relation:

$$\begin{aligned} \gamma^3 + \gamma^2 \left( \eta_B k_Z^2 + 3\nu \frac{m^2}{R^2} \right) + \gamma \left( \kappa^2 + 3\eta_B \nu k_Z^2 \frac{m^2}{R^2} \right) + \\ + \eta_B k_Z^2 \kappa^2 + 3\nu \frac{m^2}{R^2} \frac{d\Omega^2}{d \ln R} = 0. \end{aligned} \quad (63)$$

There can be no instability unless the constant term is negative, which requires the inequality (62) to hold. The asymptotic regime of validity for this condition is thus

$$1 \ll \frac{k_Z R}{m} \ll (3\mathcal{P})^{1/2}. \quad (64)$$

There are further restrictions, however, if the maximum growth rate is not to depart significantly from its value in equation (41). If we regard the dispersion relation as an equation for  $m^2/R^2$ , it may be shown that it has a well-defined solution for  $\gamma \rightarrow \gamma_{max}$ , only if

$$\eta_B k_Z^2 \ll |d\Omega^2/d \ln R|. \quad (65)$$

Similarly, if we regard the dispersion relation as an equation  $k_Z^2$ , the restriction is found to be

$$3\nu(m/R)^2 \gg |d\Omega^2/d \ln R|. \quad (66)$$

The last three equations may be combined to give the final form for the asymptotic domain of the axisymmetric dispersion relation (63) in which our solution for  $\gamma_{max}$  remains unaffected:

$$1 \ll \frac{k_Z R}{m} \ll \left( \frac{R}{m} \right) \left| \frac{1}{\eta_B} \frac{d\Omega^2}{d \ln R} \right|^{1/2} \ll (3\mathcal{P})^{1/2}. \quad (67)$$

#### 4. Discussion: Origin of Galactic Magnetic Fields.

The instability presented in this paper is generic and powerful. Its most rapidly growing behavior is exhibited at large vertical wavenumbers, and even in the presence of finite resistivity, it is not easily quenched. Long radial and azimuthal wavelengths are highly unstable, imparting large scale coherence in the disk plane already in the linear stages of instability.



In this section we discuss the possibility that this mechanism could be an important part of the process that gives rise to galactic magnetic fields.

Generally, galactic magnetic amplification processes are divided into two principal categories (Beck et al. 1996): (1) differential wind-up of a primordial field (Kulsrud 1986); and (2) dynamo amplification of a similar seed field. The latter category itself consists of at least two very distinct mechanisms; (2a) a classical  $\alpha\Omega$  dynamo (Parker 1979), and (2b) small scale turbulent amplification (Schekochihin et al. 2004). The weak field limit of these mechanisms are thought to be kinematic in nature. It is difficult to see how the process outlined in this paper could be unimportant, at least quantitatively, to any of these processes.

Simple wind-up of a seed field by differential rotation fails to incorporate properly the true dynamics of either the MRI or the magneto-viscous instability described here. Differential rotation and essentially any field geometry is highly unstable, resulting in large radial motions and ultimately MHD turbulence. The shearing of radial fields of course readily occurs, but it is not the primary amplification process of a differentially rotating system.

Traditional  $\alpha\Omega$  galactic dynamo models rely on the presence of favorable properties of interstellar turbulence to generate the required mean helicity. Curiously, these theories of magnetic field amplification generally do not incorporate weak-field MHD instabilities, despite the latter’s obvious potential benefits (e.g. Brandenburg et al. 1995; Hawley, Gammie, & Balbus 1996). Conversely, without something like the MRI or the magneto-viscous instability, it is not so obvious that turbulence will generally amplify the field, at least at low to moderate values of  $\mathcal{P}$ . An example of dissipative behavior is seen in a simulation of Hawley et al. (1996). The combination of hydrodynamical shear-layer turbulence plus a magnetic field lead not to dynamo activity, but to field energy loss. This result emerged despite the fact that calculation was done not in the kinematic limit, but fully in the MHD regime. However, the combination of local Coriolis, tidal, and Lorentz forces dramatically altered the dynamo properties of the ensuing turbulence: rapid and significant field amplification was observed, driven by the MRI turbulence, in a hydrodynamically stable background.

More recently, the notion that non-helical homogeneous small scale turbulence may play a key role in galactic dynamos, particularly in the early stages, has been investigated in a series of numerical simulations (Schekochihin et al. 2004; see also Zeldovich et al. 1984, Kulsrud & Anderson 1992), which include a scalar viscosity and study the non-kinematical regime. The idea is that certain magnetic field configurations (termed “winning” by Schekochihin et al.) align themselves smoothly with the stretching direction of the strain tensor of the turbulent flow, but fluctuate along the corresponding null axis, so that the work done on the field by fluid element stretching is not undone by relaxation. A sort of turbulent ratchet thereby ensues, growing the field with enormous efficiency at small scales.

Numerical simulations of homogeneous white noise forcing conducted by Schekochihin et al. 2004 resulted in exponential field amplification, but, interestingly, only in the regime of large  $\mathcal{P}$ . What the relationship is between these small scale structures and a galactic scale field has yet to be established.

Further discussion of the pros and cons of this mechanism would take us too far afield, but we may note that the generation of coherent magnetic field structure on scales larger than the disk scale height requires time scales at least as long as  $1/\Omega$ . And while it may well be that intrinsic interstellar turbulence plays a role in the amplification of galactic magnetic fields, we emphasize here a phenomenon that is certainly unavoidable: differential rotation. In fact, there is no reason to restrict oneself to galactic radius scales: if sub-galactic, differentially rotating turbulent vortices are also present, magneto-viscous modes should be seen on these scales as well. The key point is that a kinematic approach will miss this process, which is intrinsically MHD.

One compelling origin of the seed field for the galactic amplification process is the stars themselves (Biermann 1950, Rees 1993), in which both battery processes and a truly powerful, rapid dynamo are likely to be present. A 0.1 G azimuthal surface field diluted in a stellar wind to interstellar scales would give rise to a seed field of  $\sim 2 \times 10^{-9}$  G. With  $T \simeq 10^4$  K,  $n \simeq 1 \text{ cm}^{-3}$ , one finds

$$\omega_{ci}\tau_{ci} \simeq 10, \quad \mathcal{P} \sim 10^{11}$$

and the regime of the magneto-viscous instability is valid. The ratio of gas pressure to magnetic pressure is  $3.5 \times 10^7$ , an extremely weak field by this measure. The linear amplification factor per orbit of the magnetic energy, as noted in §3.2, is huge:  $5.2 \times 10^7$ . The makings of an MHD dynamo would seem to be present.

If a combination of magneto-viscous and magneto-rotational processes is to be a viable candidate for galactic field production, it needs to be shown that (1) the bulk of the field energy emerges in the largest scales; and (2) the saturated field energy density can grow to levels comparable to the thermal pressure. Definitive answers will require a numerical treatment, but in the meantime the following points may be considered.

A magnetic energy spectrum dominated by the largest scales appears to be a universal outcome of MRI simulations (e.g. Hawley, Gammie, & Balbus 1995), despite the fact that the most unstable modes occur at scales much smaller than the scale height. In such calculations, the available dynamical range is limited. To the extent it can be measured, however, the inertial range is Kolmogorov-like in the magnetic energy. In hydrodynamics, Kolmogorov scaling for the kinetic energy power spectrum is universal, if the dissipation rate per unit volume is the sole constant characterizing the cascade, as often seems to be the case.

Universal processes may also be at work in MHD turbulence (Kraichnan 1963; Goldreich & Sridhar 1997). An important caveat, however, is that most MHD turbulence studies have been based on wave-wave interactions (which may be of secondary importance in linearly unstable rotating systems), and they have yet to address the role of a magnetized viscosity.

Indeed, a magnetized viscosity may be crucial to understanding why interstellar fields are thermal strength (or even slightly above), whereas all numerical MRI simulations to date have yielded subthermal saturated field strengths. It has been argued (Balbus & Hawley 1998) that the outcome may be well be sensitive to  $\mathcal{P}$ . The point is that large scale reconnection proceeds relatively easily in simulations when the resistive scale is comparable to or larger than the viscous scale. In “ideal MHD,” both scales are grid based. But matters are likely to be very different if the viscous scale is, say, five orders of magnitude larger. In that case, enormous viscous stresses would occur in the course of setting up a reconnection front, and prevent its formation. With reconnection stifled, MHD turbulence could amplify the field to its natural dynamical limit: the thermal energy density. Beyond this point, buoyant effects would make it difficult for a suprathermal field to remain in the disk and be further amplified (Parker 1979).

Large Prandtl number simulations have in fact recently begun (Schekochihin et al. 2004), and treatments of the anisotropic Braginskii viscosity and conductivity have yet to be attempted. With the resistivity scale hidden below the viscous dissipation scale, there is no effective small scale sink for the magnetic field, and is therefore not surprising to note that Schekochihin et al. find that the magnetic energy spectra increases with wave number on subviscous scales, before it is ultimately cut-off. By way of sharp contrast, the ideal MRI simulations noted above find a monotonically decreasing energy spectrum for the magnetic field (Hawley, Gammie, & Balbus 1995).

The magneto-viscous instability is a powerful and general mechanism to amplify weak magnetic fields in galaxies, or in hot dilute plasmas more generally, and is worthy of more detailed study. Of particular interest would be a suite of numerical simulations designed to isolate the differences between high Prandtl number turbulent dynamos relying on MHD and differential rotation, those based on random forcing only, and those containing both.

## 5. Summary

When the ion Larmor radius is less than its collisional mean free path, the form of the viscosity is altered. Crudely speaking, angular momentum is transported only along magnetic lines of force. This causes conjoined fluid elements in a differentially rotating system to

separate radially, dragging field lines with them. This aligns the field lines along the angular velocity gradient, causing an increase in the diffusive angular momentum transport, and the process is highly unstable. The instability has previously been studied in its plasma kinetic guise (Quataert et al. 2002; Sharma et al. 2003), and we find quantitative agreement in areas of overlap with this approach. The magneto-viscous instability does not rely directly upon magnetic stresses; the field serves merely to channel angular momentum transport along its lines of force. This is effective even at exceedingly weak magnetic field strengths. The maximum growth rate of the instability is given by equation (41), and exceeds the Oort-A value of any disk stable by the hydrodynamical Rayleigh criterion. Numerical simulation of the nonlinear resolution of the instability promises to be a challenging problem. Preliminary studies on the related magneto-thermal instability, have, in fact, begun (J. Stone 2004, private communication).

The long mean free path regime is appropriate to nonradiative accretion flows around black holes (Quataert et al. 2002; Sharma et al. 2003), or to the interstellar medium of disk galaxies, our interest in this work. The magneto-viscous instability is thus a candidate for amplifying very small galactic seed fields into thermal strength fields. The turbulent MHD power spectrum, if it may be extrapolated from the moderately resolved, relatively low Prandtl number regime of previous examples, would evidence most of the power on large scales. On the other hand, the large Prandtl number regime, which characterizes the interstellar medium, ensures that the resistive dissipation scale is much smaller than the viscous scale. This may make it possible to grow thermal strength magnetic fields, despite the subthermal fields obtained in numerical MRI simulations, which correspond to the opposite Prandtl regime. But, at the same time, it is possible that the high Prandtl number regime may skew the power spectrum toward smaller scales (Schekochihin et al. 2004).

A very general gasdynamical investigation of the instability, including its behavior for arbitrary wavenumber directions, and the dynamical stress of field line tension, will be presented in a forthcoming paper (Islam & Balbus 2004, in preparation).

### Acknowledgements

I would like to thank the referees G.W. Hammett and E. Quataert for an extremely constructive and thoroughgoing review. I am also grateful to T. Islam for useful discussions, to S. Cowley, J. Stone, and A. Schekochihin for comments on an earlier draft of this work, and to the Ecole Normale Supérieure for providing financial support and a stimulating atmosphere, which fostered the completion of this work. Support from NASA grants NAG5–13288 and NAG5–9266 is gratefully acknowledged.

## REFERENCES

- Balbus, S. A. 2001, *ApJ*, 562, 909
- Balbus, S. A. 2003, *ARA&A*, 41, 555
- Balbus, S. A., & Hawley, J. F. 1992, *ApJ*, 400, 610
- Balbus, S. A., & Hawley, J. F. 1998, *Rev. Mod. Phys.*, 70, 1
- Beck, R., Brandenburg, A., Moss, D., Shukurov, A., & Sokoloff, D. 1996, *ARA&A*, 34, 155
- Biermann, L. 1950, *Z. Naturforsch.*, 5a, 65
- Braginskii, S. I. 1965, *Reviews of Plasma Physics*, New York: Consultants Bureau Enterprises, 1, 205
- Brandenburg, A., Nordlund, Å., Stein, R. F., & Torkelsson, U. 1995, *ApJ*, 446, 741
- Goldreich, P., & Lynden-Bell, D. 1965, *MNRAS*, 130, 125
- Goldreich, P., & Sridhar, S. 1997, *ApJ*, 485, 680
- Hawley, J. F., Gammie, C. F., & Balbus, S. A. 1995, *ApJ*, 440, 742
- Hawley, J. F., Gammie, C. F., & Balbus, S. A. 1996, *ApJ*, 464, 690
- Kraichnan, R. 1963, *Phys. Fluids*, 6, 1603
- Kulsrud, R. 1986, in *Plasma Astrophysics*, T. D. Guyenne & L. M. Zeleny, Paris: ESA Publ. SP-251, 531
- Kulsrud, R. M., & Anderson, S. W. 1992, *ApJ*, 396, 606
- Malayshkin, L., & Kulsrud, R. 2002, *ApJ*, 571, 619
- Menou, K., Balbus, S. A., & Spruit, H. 2004, *ApJ*, 607, in press
- Parker, E. 1979, *Cosmical Magnetic Fields*, Oxford: Oxford Univ. Press
- Quataert, E., Dorland, W., & Hammett, G. W. 2002, *ApJ*, 577, 524
- Rees, M. J. 1993, in *Cosmical Magnetism*, D. Lynden-Bell, Dordrecht: Kluwer, 155
- Sharma, P., Hammett, G., & Quataert, E. 2003, *ApJ*, 596, 1121

- Schekochihin, A., Cowley, S. C., Taylor, S. F., Maron, J. L., & McWilliams, J. C. 2004, ApJ, in press ApJ, in press (astro-ph/03012046 v2)
- Snyder, P. B., Hammett, G. W., & Dorland, W. 1997, Phys. Plasmas, 4, 3974
- Spitzer, L. 1962, Physics of Fully Ionized Gases, New York: Wiley
- Zeldovich, Ya. B., Ruzmaikin, A. A., Molchanov, S. A., & Sokoloff, D. D. 1984, J. Fluid Mech., 144, 1